TOMOGRAPHY AND METHODS OF TRAVEL-TIME CALCULATION FOR REGIONAL SEISMIC LOCATION

Stephen C. Myers[1], Sanford Ballard[2], Charlotte A. Rowe[3], Gregory S. Wagner[4], Michael S. Antolik[5], W. Scott Phillips[2], Abe L. Ramirez[1], Mike L. Begnaud[2], Mike E. Pasyanos[1], Doug A. Dodge[1], Megan P. Flanagan[1], Kevin D. Hutchenson[5], Glenn T. Barker[2], John J. Dwyer[4], and David R. Russell[4]

Lawrence Livermore National Laboratory[1], Sandia National Laboratory[2], Los Alamos National Laboratory[3], Air Force Technical Applications Center[4], Quantum Technology Sciences, Inc.[5]

ABSTRACT

We are developing a laterally variable velocity model of the crust and upper mantle across Eurasia and North Africa to reduce event location error by improving regional travel time prediction accuracy. The model includes both P and S velocities, and we describe methods to compute travel times for Pn, Sn, Pg, and Lg phases. For crustal phases Pg and Lg we assume that the waves travel laterally at mid-crustal depth, with added ray segments from the station/event to the mid crustal layer. Our work on Pn and Sn travel times extends the methods described by Zhao and Xie (1993). With consideration for a continent-scale model and application to seismic location, we extend the model parameterization of Zhao and Xie (1993) by allowing the upper-mantle velocity gradient to vary laterally. This extension is needed to accommodate the large variation in gradient that is known to exist across Eurasia and North Africa. Further, we extend the linear travel-time calculation method to mantle-depth events, which is needed for seismic locators that test many epicenters and depths. Using these methods, Sandia National Laboratory has developed a code to compute regional travel times on-the-fly from the velocity model in milliseconds, forming the basis of a flexible travel-time facility that may be implemented in an interactive locator.

We use a tomographic technique to improve upon a laterally variable starting velocity model that is based on Lawrence Livermore and Los Alamos National Laboratory model compilation efforts. Our tomographic data set consists of approximately 20 million regional arrivals from events that meet the ground truth (GT) criteria of Bondar et al. (2004) and other non-seismic constraints. Each datum is tested to meet strict quality control standards that include comparison with established distance-dependent travel time residual populations relative to the model iasp91. In addition to bulletin measurements, nearly 50 thousand arrival measurements were made at the national laboratories. The tomographic method adjusts Pn velocity, mantle gradient, and a node-specific crustal slowness correction for optimized travel-time prediction.

Report Documentation Page	*Form Approved* *OMB No. 0704-0188*

Public reporting burden for the collection of information is estimated to average 1 hour per response, including the time for reviewing instructions, searching existing data sources, gathering and maintaining the data needed, and completing and reviewing the collection of information. Send comments regarding this burden estimate or any other aspect of this collection of information, including suggestions for reducing this burden, to Washington Headquarters Services, Directorate for Information Operations and Reports, 1215 Jefferson Davis Highway, Suite 1204, Arlington VA 22202-4302. Respondents should be aware that notwithstanding any other provision of law, no person shall be subject to a penalty for failing to comply with a collection of information if it does not display a currently valid OMB control number.

1. REPORT DATE **SEP 2007**	2. REPORT TYPE	3. DATES COVERED **00-00-2007 to 00-00-2007**

4. TITLE AND SUBTITLE **Tomography and Methods of Travel-Time Calculation for Regional Seismic Location**	5a. CONTRACT NUMBER
	5b. GRANT NUMBER
	5c. PROGRAM ELEMENT NUMBER
6. AUTHOR(S)	5d. PROJECT NUMBER
	5e. TASK NUMBER
	5f. WORK UNIT NUMBER

7. PERFORMING ORGANIZATION NAME(S) AND ADDRESS(ES) **Lawrence Livermore National Laboratory,PO Box 808,Livermore,CA,94551-0808**	8. PERFORMING ORGANIZATION REPORT NUMBER

9. SPONSORING/MONITORING AGENCY NAME(S) AND ADDRESS(ES)	10. SPONSOR/MONITOR'S ACRONYM(S)
	11. SPONSOR/MONITOR'S REPORT NUMBER(S)

12. DISTRIBUTION/AVAILABILITY STATEMENT
Approved for public release; distribution unlimited

13. SUPPLEMENTARY NOTES
Proceedings of the 29th Monitoring Research Review: Ground-Based Nuclear Explosion Monitoring Technologies, 25-27 Sep 2007, Denver, CO sponsored by the National Nuclear Security Administration (NNSA) and the Air Force Research Laboratory (AFRL)

14. ABSTRACT
see report

15. SUBJECT TERMS

16. SECURITY CLASSIFICATION OF:			17. LIMITATION OF ABSTRACT	18. NUMBER OF PAGES	19a. NAME OF RESPONSIBLE PERSON
a. REPORT **unclassified**	b. ABSTRACT **unclassified**	c. THIS PAGE **unclassified**	**Same as Report (SAR)**	**10**	

Standard Form 298 (Rev. 8-98)
Prescribed by ANSI Std Z39-18

OBJECTIVES

This project produces a laterally variable velocity model of the crust and upper mantle that is specifically designed for use in routine seismic location. At this time the Seismic Location Baseline Model (SLBM) is focused on travel-time prediction at local and regional distances. Therefore, ray paths are wholly within the crust and upper mantle. Like any travel-time prediction method used in a location algorithm the SLMB must return

1. An accurate travel-time prediction and
2. An uncertainty estimate of the travel-time prediction error

Because the SLBM is meant for use in routine location algorithms where networks can be dynamic and pre-computation of travel times for all available data may not be possible, the SLBM must also

3. Compute the travel time on-the-fly given regional- or local-distance station/event coordinates and
4. Return the travel time in milliseconds, thus enabling the estimation of a location in a few seconds

Further, we aim to improve a starting model that is based on a geophysical compilation. The improvement will be achieved using a ground-truth data set and a tomographic technique that is tailored to optimize model parameters important to seismic location.

RESEARCH ACCOMPLISHED

We meet the objectives outlined above by adapting several approaches for model parameterization and travel-time calculation into one package for computation of regional- and local-distance travel times for Pn, Sn, Pg, and Lg phases.

A challenge for this project is developing a model parameterization that enables fast and accurate prediction of each local/regional phase at all applicable distances. Well-established methods can be used to compute regional Pn and Sn travel times (e.g., Hearn, 1984), but the accuracy of these methods degrades at far regional (>1000 km) distance (e.g., Hearn et al., 2004). To more accurately predict Pn and Sn at far-regional distances, Zhao (1993) and Zhao and Xie (1993) approximate upper-mantle structure with a linear gradient, resulting in a simple expression for calculating travel time. For Pn and Sn, we adapt the Zhao and Xie (1993) approach for application to seismic location. For Pg and Lg (Sg) at local distances, we extract a vertical cross section from the model and use 2-dimensional ray tracing to compute the travel time. At regional distance, we approximate the crustal waveguide (Pg and Lg phases) with a laterally variable velocity layer, while accounting for propagation to/from the station/event using ray tracing.

In each instance we use tomographic methods to improve travel-time prediction of the model. Lawrence Livermore and Los Alamos National Laboratories (LLNL and LANL, respectively) are developing a joint ground truth data set for tomography that includes stringent quality control measures for arrival-time measurements. We adapt Pn tomographic methods (e.g., Hearn 2004; Zhao and Xie, 1993, Phillips et al., 2007) to improve travel-time predictions of each regional phase.

Model Parameterization

We combine the laterally variable layer approach of Pasyanos et al. (2004) with the linear mantle gradient of Zhao and Xie (1993). Layer definitions are specified in Table 1. Note that the thickness of some layers may be zero. For instance, on the continents the depth of the water layer coincides with the depth of the model layer exposed at the surface. Velocity vs. depth profiles are defined at nodes, and the profiles at the nodes are interpolated using an efficient code developed at Sandia National Laboratory (SNL) to determine velocity at any arbitrary location (lat,lon,depth). SNL has also developed a tessellation node structure on a spheroid with node spacing of approximately 1° (Figure 1). At present, the model development domain is Eurasia and North Africa, and nodes inside that domain capture the effects of 3-dimensional structure on travel times. Outside of the development domain nodes are set to a default velocity profile based on iasp91 (Kennett and Engdahl, 1991). This parameterization provides a seamless and extensible model. Expansion beyond Eurasia and North Africa does not require a change in the model parameterization itself, only modification of the velocity structure at previously defined nodes. Further, SNL has incorporated the GRS80 ellipsoid in to the model, eliminating the need for the conventional ellipticity correction to travel-time predictions.
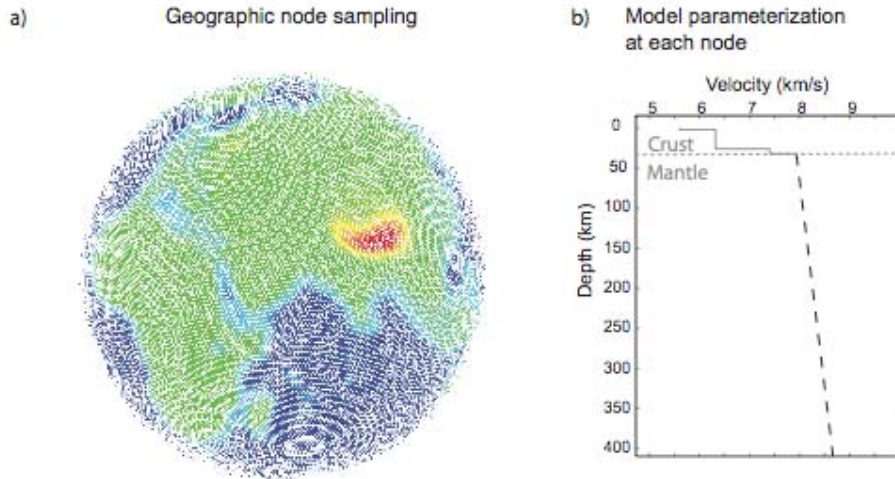
Figure 1. SLBM global parameterization. a) An example tessellation with approximately 1° grid spacing. Color is based on approximate Moho depth. b) An example velocity/depth profile as defined at each node. The mantle portion of the profile is specified by the velocity at the crust/mantle interface and a linear gradient.

Table 1. Model entities and associated parameters. Depths and velocities at each node are interpolated to define a 3-dimensional crustal model that overlies a laterally variable model in the shallow mantle. Note that the mid-crustal layer is distinct, in that the velocities are specified individually for each phase. For Pn and Sn the mid-crustal layer is used in conjunction with all other crustal layers to compute travel times for rays that travel steeply through the crust. For Pg and Lg distinct middle crust velocities are used to model the horizontal slowness of the regional phases that are trapped in the crust.

Model entity	Layer Depth	P-wave velocity	S-wave velocity	P-wave gradient	S-wave gradient
Water	Yes	Yes	Yes		
Sediment 1	Yes	Yes	Yes		
Sediment 2	Yes	Yes	Yes		
Sediment 3	Yes	Yes	Yes		
Upper Crust	Yes	Yes	Yes		
Middle Crust	Yes	Independent for Pn, Pg	Independent for Sn, Lg		
Lower Crust	Yes	Yes	Yes		
Moho	Yes	Yes	Yes		
Mantle Gradient				Yes	Yes

Travel-Time Calculation, Pn and Sn

The travel-time calculation is based on the method described in Zhao (1993) and Zhao and Xie (1993). This calculation is similar to the widely used approach of Hearn (1984), with an additional term (γ) introduced to account for diving rays that may occur due to a positive velocity gradient with depth and Earth sphericity.

416

The travel-time calculation is

$$TT = \sum_{i=1}^{N} d_i s_i + \alpha + \beta + \gamma \qquad [1]$$

where d and s are the distance and slowness (taken as 1/MohoVelocity) in each of the i segments comprising the great-circle path between Moho pierce points near the station/event, α and β are the crustal travel times at the source and receiver, and γ is a term that accounts for the effect of both mantle velocity gradient and earth sphericity.

We define α as

$$\alpha = \sum_{j=1}^{M} \left[\sqrt{r_j^2 / v_j^2 - p^2} - \sqrt{r_{j+1}^2 / v_j^2 - p^2} \right] \qquad [2]$$

where v and r are the velocity and layer radius of the M crustal layers from the event to the Moho, and p is the ray parameter ($p=1/v$, v evaluated at the ray bottoming depth).

We similarly define β as

$$\beta = \sum_{k=1}^{N} \left[\sqrt{r_k^2 / v_k^2 - p^2} - \sqrt{r_{k+1}^2 / v_k^2 - p^2} \right] \qquad [3]$$

where v and r are defined as above for the L crustal layers from the station to the Moho. The same p is used in both Eqns [2] and [3]. Because the ray bottoming depth is a function of the pierce point, p is determined through an efficient, iterative process.

Per Zhao and Xie (1993),

$$\gamma = -\frac{c^2 Xm^3}{24 V_0} \qquad [4]$$

where X_m is the horizontal distance traveled in the mantle, c is a velocity gradient in the mantle that is normalized by the velocity at the crust mantle boundary plus an additional term to account for Earth sphericity (Helmberger, 1973), and V_0 is a regional average of Pn velocity over the entire study area.

We introduce spatially varying c into the model (Phillips et al., 2007), and we calculate γ by averaging c along each ray. V_0 remains an average Pn velocity over the whole model, which allows us to take advantage of linear tomographic inversion methods (see below). Tests suggest that the approximation to V_0 introduces negligible travel-time error given Pn velocities ranging from 7.5 km/s to 8.3 km/s.

The Zhao (1993) method is applicable to events in the crust, making the approach well suited to nuclear explosion monitoring. However, seismic location algorithms may explore the possibility that an event occurred in the mantle, necessitating a consistent method of travel-time predictions for mantle events. The following extends the travel-time method to events in the shallow mantle, with the condition that $c^2h^2 \ll 1$ (h is the bottoming depth of the ray)

$$TT = \alpha + t_m \qquad [5]$$

where α is the crustal travel time from the Moho to the station (as defined in [2]), and t_m is the travel time in the mantle. Figure 2 shows the geometry and defines many of the variables used in the following equation.

$$t_m = \frac{\left[t_{Moho} \frac{x_m}{d} - \left(\frac{c^2 x_m^2}{24 V_0} \right) \right] \pm \left[t_{Moho} \left(\frac{x_z}{d(1+c_m z_m)} \right) - \left(\frac{c^2 x_z^2}{24 V_{0z}} \right) \right]}{2} \qquad [6]$$

If the ray leaves the event upwards, then the second term is subtracted. If the ray leaves the event downwards, then the second term is added. t_{Moho} is the travel time for a ray traversing the Moho from the event to the point where the ray enters the crust and propagates to the station. x_m is the horizontal distance as measured at Moho radius by a ray that starts at the Moho then travels downward passing through the event and continuing to the station. x_z is similar to x_m, but the horizontal distance is measured at the radius of the event. d is the horizontal distance traveled in the mantle from the event to the Moho pierce point below the station, as measured at Moho radius. c_m is the mantle velocity gradient normalized by average Moho velocity, with the addition of a term to account for earth sphericity

(Helmberger, 1973). z_m is the depth of the event below the Moho. V_{oz} is the average model velocity at the depth of the event.
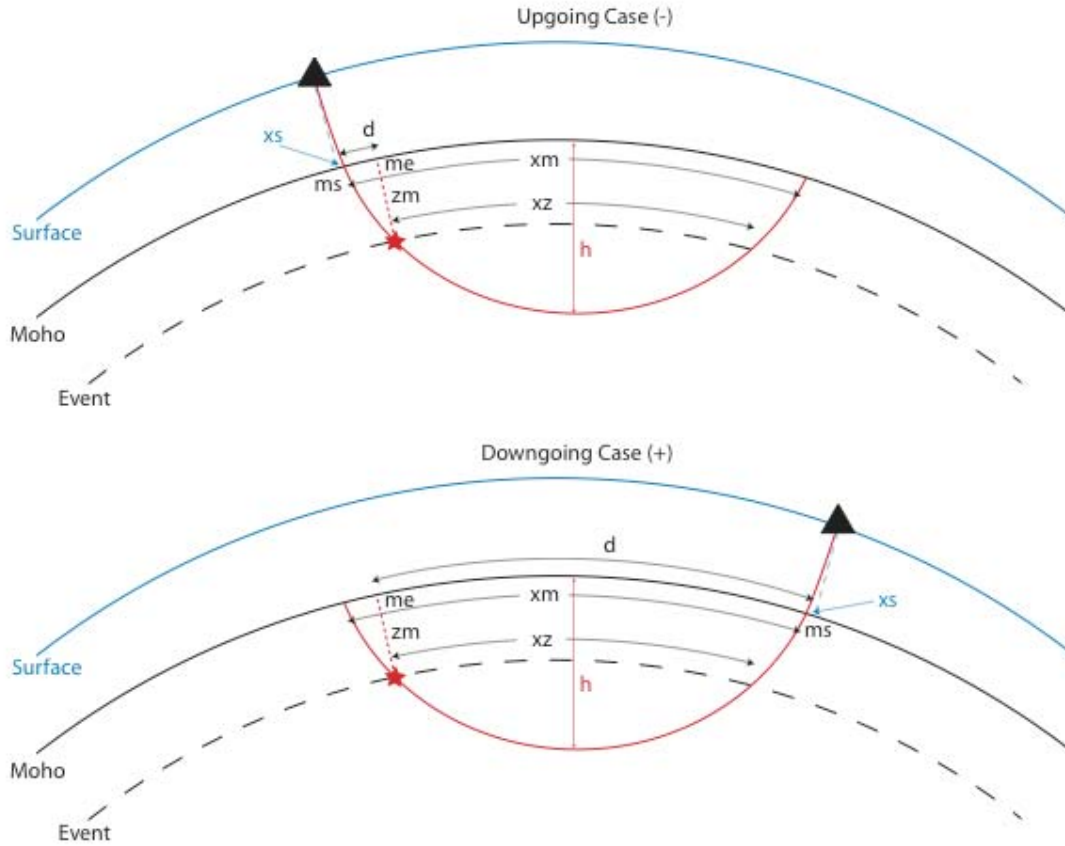

Figure 2. Geometry and variable definition extending the Zhao and Xie (1993) formulation to events in the shallow mantle. The red star is the event location and the triangle is the station location.

Travel-Time Calculation, Pg and Lg

Both Pg and Lg phases are trapped in the crust, and both phases exhibit complex waveforms that require hundreds or thousands of rays to model. Further, the first arriving ray with sufficient energy to be observed is dependent on geologic structure and station/event distance. Therefore, it is difficult to physically model the observed travel time using conventional ray techniques. Empirically, Pg and Lg travel at horizontal velocities of approximately 6.0 km/s and 3.2 km/s (respectively), which is suggestive of propagation in the middle crust. Further, event depth can impart a static travel-time delay, suggesting a component of propagation from the event to the middle crust then up to the station. We capture this travel-time behavior with a simple approximation whereby:

$$TT = \sum_{i=1}^{N} d_i s_i + \alpha + \beta \qquad [7]$$

where d_i is the distance traveled in the middle crust in each of N ray segments and α and β propagate the phase to and from the middle crust, respectively. When the source is above the middle crust, then the calculation is almost the same as [1], but the correction for a diving ray is not used. When the source is below the mid-crustal layer, we assume that the ray travels horizontally until Earth sphericity causes the ray to intersect the mid-crustal layer. While this approach by no means captures the physical complexity of Pg and Lg wave propagation, we find that it is suitable for estimating travel time.

Computational Efficiency

Travel-time facilities used in routine location algorithms must be computationally efficient. Analysts often iterate on arrival-time measurements, first locating the event with clear arrivals, then adding additional arrivals (or adjusting previous measurements) based on a preliminary location. The demands of routine seismic analysis preclude waiting more than a second or two for the calculation of a location before continuing work. Considering that a location requires the computation of travel times for many phases, over many iterations, often with numerical calculation of derivatives (at least 4 travel-time calculations per observation per iteration), the time to compute an individual travel time must be negligible (milliseconds).

The algebraic form of the travel-time formulas that are specified above consume negligible computer time. The primary challenge is fast extraction of the cross sectional profile needed for the travel-time calculation from the laterally variable model. The tessellation model parameterization developed at SNL takes advantage of mature algorithms to determine which triangle any given point lies within, which nodes comprise the triangle, and node weights used for interpolation. Figure 3 shows an example of a cross section and the Pn ray that is used to compute the travel time.

Test results show a linear increase in computer time as a function of station/event distance. In the distance range from ~200 km to ~2200 km, Pn/Sn travel times require ~1 milliseconds to 2 milliseconds to compute on a desktop computer with ~1.5Ghz clock speed. Pg/Lg times are faster.
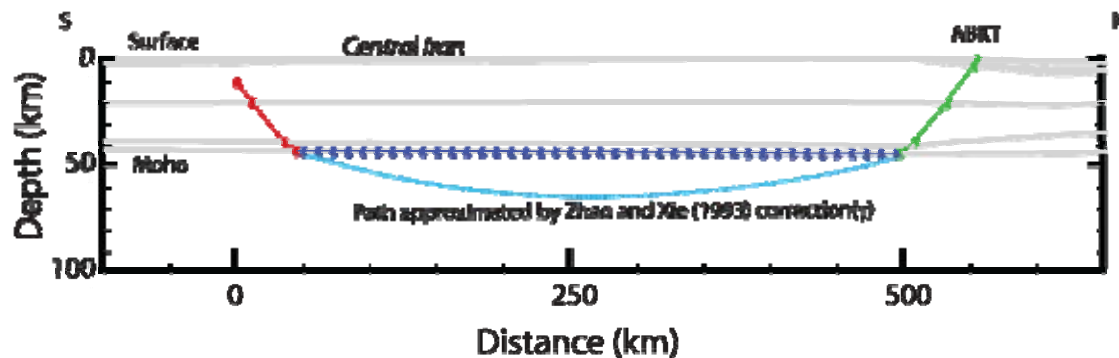

Figure 3. Cross section extracted from the laterally variable SLBM model. The components of the Pn/Sn travel-time calculation are also shown. The blue, red, green, and cyan colors correspond to the first, second, third, and fourth terms of Eqn 1.

Travel-Time Accuracy

We make use of many approximations to meet the challenge of fast, on-the-fly travel-time calculation. We test the accuracy of these calculations by comparing travel times computed using the methods described above (SLBM) with travel times computed using a fully 3-dimensional calculation described in Flanagan et al. (2007). The Flanagan et al. (2007) study uses the WENA1.0, 3-dimensional model of Pasyanos et al. (2004). For testing purposes, we use the WENA1.0 crustal model and mantle velocity at the Moho discontinuity. We then compute the linear mantle gradient using the velocity at the Moho and the velocity at 130 km depth.

Figure 4 shows representative results of our tests. Figure 4a,b shows the difference in Pn travel times computed using the SLBM method and using 3-dimensional finite difference, respectively. In both cases the comparisons are relative to the iasp91 model, and Pn travel times are computed using the TauP toolkit of Crotwell et al. (1999). The general features of Figure 4a and 4b are similar, with deviations from iasp91 travel times ranging from approximately 2 seconds late to 6 seconds early. Figure 4c shows the difference between the SLBM and finite-difference calculations, with deviations between the two methods generally between plus and minus 1 second. Errors in the finite difference calculations themselves are reported to be approximately plus and minus 0.5 seconds (Flanagan et al., 2007). These tests suggest that the efficient SLBM computational errors are slightly larger than the computationally demanding finite-differences calculations, and SLBM errors are relatively small compared to iasp91 travel-time anomalies.
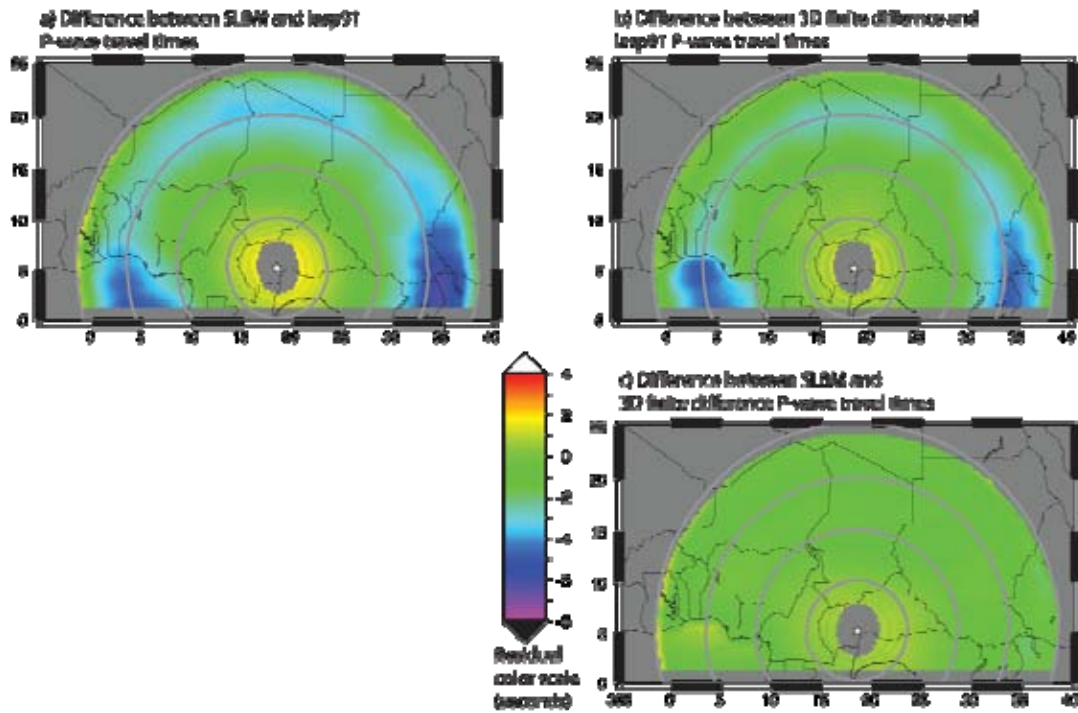
Figure 4. Comparision of Pn travel times using SLBM and 3D finite difference calculations for station BGCA in central Africa. For SLBM and 3D finite-difference calculations the WENA1.0 model of Pasyanos et al. (2004) is used. Circles around the station are 5° increments. See text details.

Tomography

Test results presented above suggest that the SLBM travel-time method is in good agreement with 3-dimensional calculations. The WENA1.0 model used in the tests above is shown to improve travel-time prediction and location accuracy relative to the iasp91 default model (Flanagan et al., 2007). We will further improve SLBM travel-time accuracy using tomographic methods.

A data set with small errors in event location and arrival-time measurements is critical to tomographic studies. Data coverage is also critically important. LLNL and LANL have combined ground-truth data sets for this study. Both national laboratories contribute global, regional, and local bulletins (some not widely available), as well as tens of thousands of arrival-time measurements made at the national laboratories. All event locations are evaluated against Bondar et al. (2004) epicenter accuracy criteria, and all picks are evaluated against an error budget that accounts for event mislocation, iasp91 prediction error, and arrival-time measurement error. Observations outside of the 99% confidence bounds for total error are removed. Figure 5 shows the extensive data coverage for Pn, Sn, Pg, and Lg throughout Eurasia.

We are using the SLBM travel-time calculator in tomographic inversion programs. The general form of the tomographic inversion for Pn/Sn is as follows:

$$T^k = \sum_{i=1}^{N} s_i^k x_i^k + \frac{\left(c^k\right)^2 \left(X_m^k\right)^3}{24 V_0} + \sum_{j=1}^{N} a_j^k \sum_{p=1}^{Q} \frac{l_p^k}{v_p^k} \qquad [8]$$

A significant difference between the formulation presented here and more typical Pn-tomography formulations is the introduction of a scalar value that adjusts the slowness of the crustal stack, as opposed to a static time-term to

account for crustal travel-time delays. Adjusting the crustal slowness produces a model that is better suited to account for the effects of event depth on predicted travel times and therefore better for estimating event depth.

The tomographic free parameters are more easily identified in matrix form:

$$
\begin{bmatrix}
x_1^1 & \cdots & x_N^1 & -\dfrac{x_1^1(X_m)^3}{24V_oX_m} & \cdots & -\dfrac{x_N^1(X_m)^3}{24V_oX_m} & \sum\limits_{p=1}^{Q}\dfrac{l_{1p}^1}{v1p} & \cdots & \sum\limits_{p=1}^{Q}\dfrac{l_{Np}^1}{vNp} \\
\vdots & & & & \ddots & & & & \vdots \\
x_1^K & \cdots & x_N^K & -\dfrac{x_1^K(X_m)^3}{24V_oX_m} & \cdots & -\dfrac{x_N^K(X_m)^3}{24V_oX_m} & \sum\limits_{p=1}^{Q}\dfrac{l_{1p}^K}{v1p} & \cdots & \sum\limits_{p=1}^{Q}\dfrac{l_{Np}^K}{vNp} \\
& & & & \text{Re}\,gularization & & & &
\end{bmatrix}
*
\begin{bmatrix}
s1 \\ \vdots \\ sN \\ c_1^2 \\ \vdots \\ c_N^2 \\ a1 \\ \vdots \\ aN
\end{bmatrix}
=
\begin{bmatrix}
T^1 \\ \vdots \\ T^K \\ \text{Re}\,gularization
\end{bmatrix}
\quad [9]
$$

where

T = travel time,
s = Pn slowness,
x = Pn distance (or weight),
c = normalized velocity gradient v=vo(1+cz),
X_m = length of Pn path,
V_o = average Pn velocity,
v = velocity of a crustal layer,
k = index on K paths (travel-time observations),
i = index on N model nodes (mantle path),
j = index on N model nodes (crustal path),
p = index on Q crustal layers, and
a = scalar adjustment to the crustal
          slowness stack at each node.

CONCLUSIONS AND RECOMMENDATIONS

We describe the progress of the SLBM project to date. This project is distinct because it tailors the travel-time prediction algorithm and tomography results for use in routine seismic location algorithms. Emphasis is placed on travel-time prediction accuracy and computational efficiency of regional phases.

The tessellation model parameterization provides seamless global coverage. The use of a tessellation approach also allows fast interpolation of model parameters to extract the great-circle cross section of velocity structure that is needed to compute regional travel times. The current focus of the SLBM effort is Eurasia and North Africa, and model nodes outside of that area are set to a default velocity structure based on the iasp91 model (Kennett and Engdahl, 1991). We note that the model is extensible, and a global calibration effort would entail updating node-centered velocity profiles (by whatever means), which does not require updates to the model tessellation or travel-time codes.
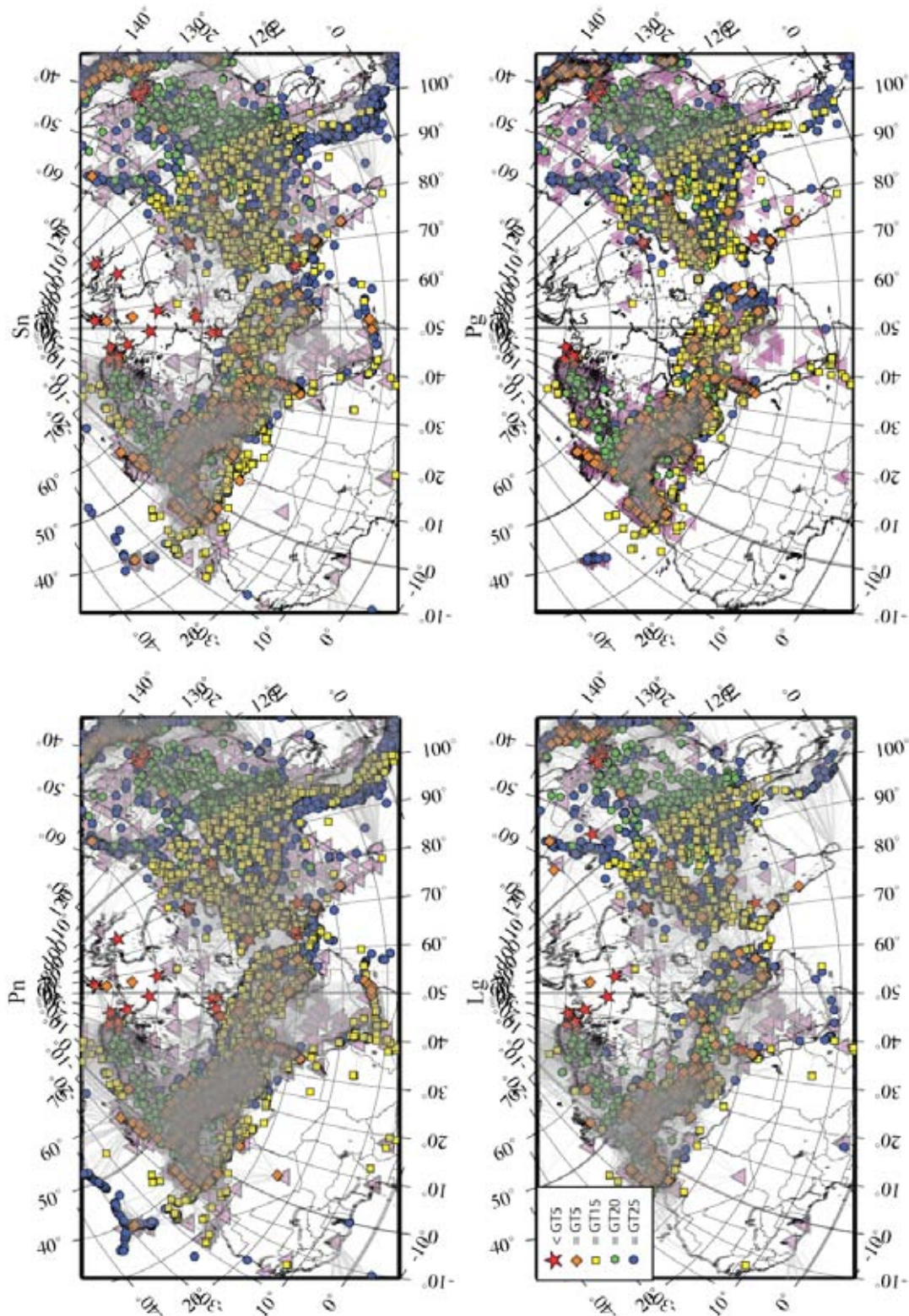
Figure 5. Tomographic data set. Purple triangles are stations with at least 1 regional-distance arrival-time measurement. Ground-truth location and accuracy (as defined in Bondar et al., 2004) are shown in the legend in the lower left. Regional ray coverage (shown by gray lines) is excellent throughout the study area, with the exception of North Africa.

We make use of several approximations that result in a relatively simple algebraic form for travel-time calculations. We have tested the accuracy of the approximate methods against full, 3-dimensional finite-difference calculations. The differences between the approximate methods and full, 3-dimensional finite-difference methods are estimated to be less than 10% of errors observed by using a simple iasp91 background model. Therefore, we conclude that the approach developed here is a significant improvement in routine location practice.

We have developed an extensive, quality-controlled, ground-truth data set across Eurasia and North Africa. This data set will be used in tomographic codes that employ the SLBM travel-time calculator to further optimize the model parameters that are most important to seismic location.

ACKNOWLEDGEMENTS

REFERENCES

Bondar, I., S. Myers, E. R. Engdahl, and E. Bergman, (2004). Epicenter accuracy based on seismic network criteria, *Geophys. J. Int.* 156: no. 3, 483–496.

Flanagan, M. P., S. C. Myers, and K. D. Koper (2007). Regional travel time uncertainty and seismic location improvement using a three-dimensional a priori velocity model, *Bull. Seismolog. Soc. Am.* 97: 804–825.

Crotwell, H. P., T. J. Owens, and J. Ritsema (1999). The TauP ToolKit: flexible seismic travel-time and raypath utilities, *Seism. Res. Lett.* 70: 154–160.

Hearn, T. M. (1984). Pn travel times in southern California, *Jour. Geophys. Res*. 89: 1843–1855.

Hearn, T. M., S. Wang, J. F. Ni, Z. Xu, Y. Yu, and X. Zhang (2004). Uppermost mantle velocities beneath China and surrounding regions, *J. Geophys. Res*. 109: B11301, doi:10.1029/2003JB002874.

Helmberger, D.V. (1973). Numerical seismograms of long-period body waves from seventeen to forty degrees, *Bull. Seismol. Soc. Am*. 63: 633–646.

Kennett, B. L. N. and E. R. Engdahl, (1991). Traveltimes for global earthquake reference location and phase identification, *Geophys. J. Int,* 105: 429–465.

Pasyanos, M. E., W. R. Walter, M. P. Flanagan, P. Goldstein, and J. Bhattacharyya (2004). Building and testing an a priori geophysical model for western Eurasia and North Africa, *Pure. And Applied Geophys*. 161: 235–281.

Phillips, W. S., M. L. Begaud, C. A. Rowe, L. K. Steck, S. C. Myers, M. E. Pasyanos, and S. Ballard (2007). Accounting for lateral variations of the upper mantle gradient in Pn tomography studies, *Geophys. Res. Lett*., Revised.

Zhao, L.-S. (1993). Lateral variations and azimuthal isotropy of Pn velocities beneath Basin and Range province, *Jour. Geophys. Res*. 98: 22:109–22.

Zhao and Xie (1993). Lateral variations in compressional velocities beneath the Tibetan Plateau from Pn traveltime tomography, *Geophys. J. Int*. 115: 1070–1084.